

N90-17954

A CCIR AERONAUTICAL MOBILE SATELLITE REPORT

Faramaz Davarian and Dennis Bishop
Jet Propulsion Laboratory
California Institute of Technology
Pasadena, CA 91109

17p

David Rogers
Comsat Laboratories
Clarksburg, MD 20871

Ernest Smith
University of Colorado
Boulder, CO 80309-00425

The following report was prepared for and submitted to the International Radio Consultative Committee (CCIR) Study Group 5. It is intended that this report will complement the existing reports on maritime (No. 884-1) and land (No. 1009) mobile satellites.

Received:

Subject: Study Programme 7C/5
Draft New Report

United States of America

DRAFT NEW REPORT

PROPAGATION DATA FOR AERONAUTICAL MOBILE-SATELLITE SYSTEMS
FOR FREQUENCIES ABOVE 100 MHz

1. Introduction

Propagation effects in the aeronautical mobile-satellite service differ from those in the fixed-satellite service and other mobile-satellite services because:

- small antennas are used on aircraft, and the aircraft body may affect the performance of the antenna;
- high aircraft speeds cause large Doppler spreads;
- aircraft terminals must accommodate a large dynamic range in transmission and reception;
- due to their high speeds, banking maneuvers, and 3-dimensional operation, aircraft routinely require exceptionally high integrity of communications, making even short-term propagation effects very important.

This report discusses data and models specifically required to characterize the path impairments, which include:

- tropospheric effects, including gaseous attenuation, cloud and rain attenuation, fog attenuation, refraction and scintillation;
- surface reflection (multipath) effects;
- ionospheric effects such as scintillation;
- environmental effects (aircraft motion, sea state, land surface type).

Aeronautical mobile-satellite systems may operate on a worldwide basis, including propagation paths at low elevation angles. Several measurements of multipath parameters over land and sea have been conducted. In some cases, laboratory simulations are used to compare measured data and verify model parameters. The received signal is considered in terms of its possible components: a direct wave subject to atmospheric effects, and a reflected wave, which generally contains mostly a diffuse component.

In this Report, data are presented in terms of path elevation angle instead of grazing angle. For paths to geostationary satellites at elevation angles above 4° , and aircraft heights below 10 km, the maximum difference between elevation angle and grazing angle is 1° .

There is current interest in using frequencies near 1.5 GHz for aeronautical mobile-satellite systems. As most experiments have been conducted in this band, data in this report are mainly applicable to these frequencies. As aeronautical systems mature, it is anticipated that other frequencies may be used.

2. Tropospheric effects

For the aeronautical services, the height of the mobile antenna is an important parameter. Estimates of tropospheric attenuation for several antenna heights are provided in Table I.

Predictions of the 30-GHz rain attenuation exceeded for 0.1 percent of the time are shown versus aircraft height for several CCIR rain zones (§ 4.2.1 of Report 563) in Figure 1 for a path elevation angle of 10° . The model assumes surface-based terminals, and may be less accurate for airborne terminals.

The received signal may be affected both by bulk refraction and by scintillations induced by atmospheric turbulence, as discussed in Report 718. These effects may be moderated for aircraft at high altitudes. Experimental data are discussed in Report 564.

3. Ionospheric effects

Ionospheric effects on slant paths are discussed in Study Group 6 texts (see Report 263). These phenomena are important for many paths at frequencies below about 10 GHz, and are strongest within $\pm 15^\circ$ of the geomagnetic equator, and secondarily within the auroral zones and polar caps. Ionospheric effects peak near the solar sunspot maximum.

Impairments caused by the ionosphere will not diminish for the typical altitudes used by aircraft. A summary description of ionospheric effects of particular interest to mobile-satellite systems is available in § 3 of Report 884. For most communication signals, the most severe impairment will probably be ionospheric scintillation. Table I of Report 884 provides estimates of maximum expected ionospheric effects at frequencies up to 10 GHz for paths at a 30° elevation angle.

Measurements of ionospheric scintillation were conducted in one aeronautical mobile-satellite experiment [Sutton et al., 1973a]. A signal was transmitted between the ATS-5 satellite and a KC-135 aircraft parked at the Pago Pago airport (geomagnetic latitude of 17° South). During a period of severe scintillation, the peak-to-trough signal variations exceeded 4 to 6 dB, and the 1-percent fade depth approached 3.2 dB.

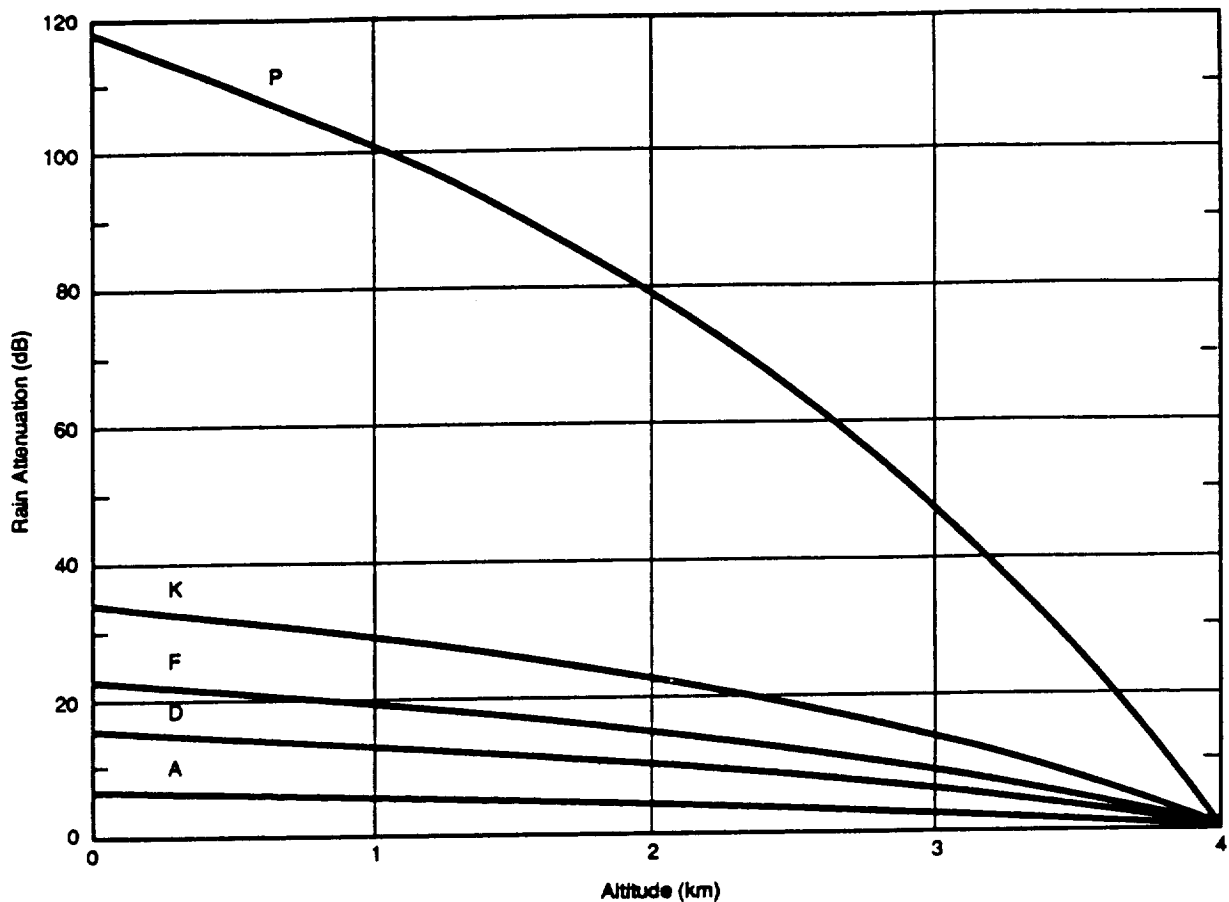


Figure 1 - Predicted 30-GHz rain attenuation at 10° elevation angle for 0.1 percent of the time vs height above sea level for several rain climate zones; latitude less than 36°

4. Fading due to surface reflection and scattering

4.1 General

Multipath fading due to surface reflections for aeronautical mobile-satellite systems differs from fading for other mobile-satellite systems because the speeds and altitudes of aircraft are much greater than those of other mobile platforms. Characteristics of fading for aeronautical systems can be analyzed with procedures similar to those for maritime systems described in Report 884, taking careful account of earth sphericity, which becomes significant with increasing antenna height above the reflecting surface [Yasunaga et al., 1986].

Table I - Estimated tropospheric attenuation for an elevation angle of 10°, one-way traversal, taking aircraft altitude into account

Effect Altitude (km)	Magnitudes (dB) for specified frequencies (GHz)					
	1.5	7.5	15	20	30	40
Oxygen attenuation ¹						
0	0.19	0.23	0.29	0.36	0.64	1.52
1	0.16	0.19	0.24	0.30	0.54	1.29
2	0.14	0.16	0.21	0.26	0.46	1.09
3	0.12	0.14	0.17	0.22	0.39	0.92
4	0.10	0.12	0.15	0.18	0.33	0.78
5	0.08	0.10	0.12	0.16	0.28	0.66
6	0.07	0.08	0.11	0.13	0.23	0.56
Water vapor attenuation ¹ (7.5 g/m ³)						
0	0.0016	0.043	0.26	1.35	0.98	1.17
1	0.0010	0.028	0.16	0.92	0.63	0.75
2	0.0006	0.018	0.11	0.62	0.40	0.47
3	0.0004	0.011	0.07	0.42	0.26	0.30
Cloud attenuation ² (1 g/m ³) (1 - 3 km ht)						
0	0.020	0.49	1.96	3.48	7.84	13.9
1	0.020	0.49	1.96	3.48	7.84	13.9
2	0.010	0.25	0.98	1.74	3.92	7.0
3	0.0	0.0	0.0	0.0	0.0	0.0
Fog attenuation ² (0.5 g/m ³) (0 - 150 m ht)						
0	0.0006	0.015	0.059	0.10	0.23	0.42
1	0.0	0.0	0.0	0.0	0.0	0.0
Rain attenuation ³ (0.1%, Zone K)						
0	0.013	2.17	11.1	18.2	34.2	47.8
1	0.011	1.86	9.5	15.5	29.2	40.9
2	0.008	1.43	7.3	11.9	22.5	31.4
3	0.005	0.80	4.1	6.7	12.5	17.5
4	0.0	0.0	0.0	0.0	0.0	0.0

¹ Derived from the method of § 2.1.1 of Report 564-3.

² Derived from models of Slobin [1982].

³ Derived from the method of § 2.2.1 of Report 564-3 for rain climate zone K (§ 4.2.1 of Report 563-3).

4.2 Fading due to sea-surface reflections

4.2.1 Dependence on antenna height and antenna gain

Figure 2 shows the calculated relationship between antenna height and 1.54-GHz multipath fading depth under rough sea conditions for an antenna gain G_θ of 10 dBi and elevation angles θ_i of 5° and 10° (Report 884, § 4), assuming the main lobe of the antenna is expressed as

$$G(\theta) = -4 \times 10^{-4} (10^{G_m/10} - 1) \theta^2 \quad (\text{dB}) \quad (1)$$

where:

G_m : value of the maximum antenna gain (dB); and

θ : angle measured from boresight (deg).

The fading depth is defined as the difference (in dB) between the signal level of the direct incident wave and the threshold level exceeded by the resultant (direct plus multipath) signal for a specified time percentage; in Figure 2 the time percentage is 99 percent. Although the fading depth decreases with increasing antenna height, the fading depth for an antenna at a height of 10 km is only 1 to 2 dB less than that for a maritime system (antenna height of the order of 10 m).

Bit-error-rate data were obtained in a flight experiment conducted over the North Atlantic using a 1.54-GHz circularly-polarized signal from a MARECS-A satellite [Zaks and Anderson, 1986]. A conformal micro-strip antenna with a 0-dBiC beamwidth of 130° was mounted on each side of the upper fuselage. The aircraft flew at a nominal height of 10.8 km and a nominal ground speed of 740 km/h. Carrier-to-multipath ratios estimated from the BER data appeared to vary from 8.5 to 13 dB over an elevation angle range of 4° to 17°.

4-5.2.2 Frequency spectrum of fading

The frequency power spectrum of sea-reflected waves depends particularly on aircraft flight speed, path elevation angle to the satellite, and the ascending (or descending) angle of the aircraft. For level flight, the frequency spectrum tends to take a symmetrical shape with a flat portion centred about the direct wave component. The -10 dB spectral bandwidth measured from the centre frequency (i.e., the frequency of the direct wave component) is about 25 Hz and 50 Hz at path elevation angles of 5° and 10°, respectively. For ascending or descending aircraft, the spectrum becomes asymmetric with the peak displaced from the centre. For example, with both elevation angle and ascending angle of 5°, the peak is about 25 Hz from the centre of the spectrum.

4-5.2.3 Delay time and coherent bandwidth (direct and reflected)

The correlation of fading between two radio waves with different frequencies decreases with increasing frequency separation. The dependence of the correlation on antenna gain is small for gains less than 15 dBi. Figure 2-3 shows the relationship between antenna height and coherent bandwidth, which is defined as the frequency separation for which the correlation coefficient between two radio waves equals 0.367 (=1/e). The coherent bandwidth decreases as the antenna height increases, becoming about 10 to 20 kHz (delay time of 6 to 12 usec) for an antenna at a height of 10 km. This means that the multipath fading for aeronautical systems may have so-called frequency-selective characteristics.

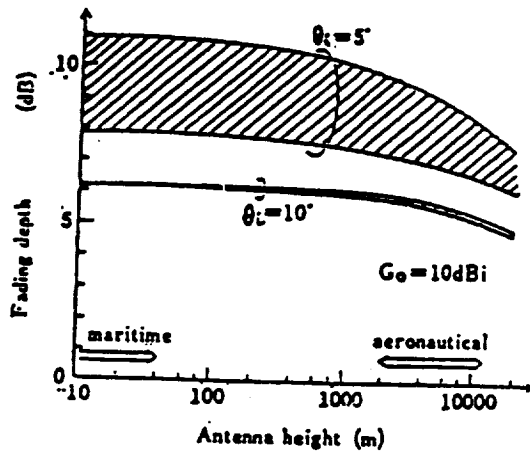


FIGURE 11- 2

Fade depth vs. antenna height for antenna gain of 10 dBi and circular polarization at 1.54 GHz under rough sea condition

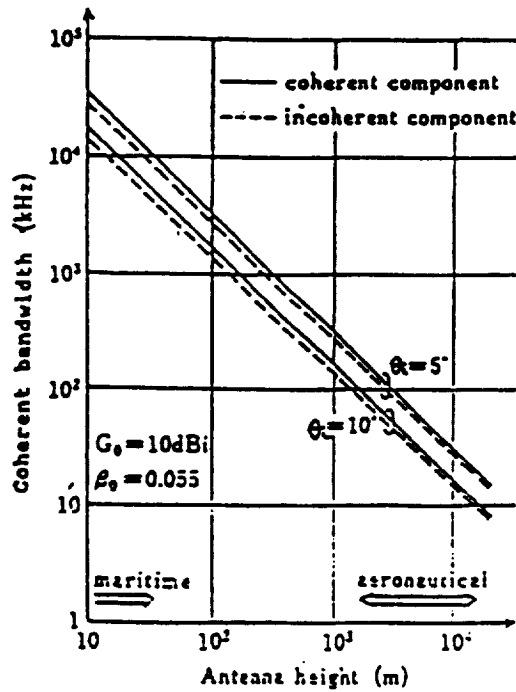


FIGURE 11- 3

Coherent bandwidth vs. antenna height for antenna gain of 10 dBi

4.3 Measurements of sea-reflection multipath effects

Extensive aeronautical multipath tests were conducted in the 1.5 to 1.6 GHz band with a KC-135 jet airplane and the NASA ATS-5 geostationary satellite [Sutton et al., 1973b]. The aircraft ground speed was 650 km/h and the orientation was generally broadside to the satellite path azimuth. The direct satellite signal was received with a 15 dBi quad-helix antenna located at the base of the vertical stabilizer; the indirect, sea-reflected signal was received with a 13 dBi crossed-dipole array.

Data were recorded during 30 over-ocean flights at elevation angles of 9° to 31° from the airplane to the satellite. Photographs of the ocean were taken (at heights of about 300 and 900 m) to determine sea surface conditions.

Measured mean multipath power normalized to the direct power (as corrected for RF channel gain differences) versus elevation angle for linear vertical and horizontal polarizations is shown in Figure 4. Each data point is derived from 6 minutes of data. Theoretical predictions are also shown (solid lines) in the figure, calculated as the product of the plane-earth reflection coefficient and the divergence factor [Staras, 1968] (see Report 1008, § 3.3).

The spectrum bandwidth (defined by the points where the spectrum amplitude is 1/e of the peak) for the sea-reflected waves is plotted versus elevation angle in Figure 5. These data were obtained by transmitting an unmodulated carrier toward the aircraft and taking the Fourier transform of the sea-reflected signal.

Another study of multipath propagation at 1.6 GHz was performed with a KC-135 aircraft and the NASA ATS-6 satellite [Schroeder et al., 1976]. The signal characteristics were measured with a two-element wave-guide array in the aircraft nose radome, with 1-dB beamwidths of 20° in azimuth and 50° in elevation. Data were collected over the ocean and over land at a nominal aircraft height of 9.1 km and nominal ground speed of 740 km/h.

Table II summarizes the oceanic multipath parameters observed in the ATS-6 measurements, augmented with results from the model [Yasunaga et al., 1986]. The delay spreads in the table are the widths of the delay-power spectral density of the diffusely-scattered signal arriving at the receiver. Coherence bandwidth is the 3-dB bandwidth of the frequency autocorrelation function (Fourier transform of the delay spectrum). Doppler spread is determined from the width of the Doppler power spectral density. The decorrelation time is the 3-dB width of the time autocorrelation function (inverse Fourier transform of the Doppler spectrum).

The mean-square scatter coefficient, Γ , in Table II is defined as

$$\Gamma = G \langle |I|^2 \rangle / \langle |D|^2 \rangle \quad (2)$$

where:

- G : adjustment to account for gain differences between the direct and indirect channels;
- $\langle |I|^2 \rangle$: mean-square power in the multipath component as measured at the receiver;
- $\langle |D|^2 \rangle$: mean-square power in the direct component as measured at the receiver.

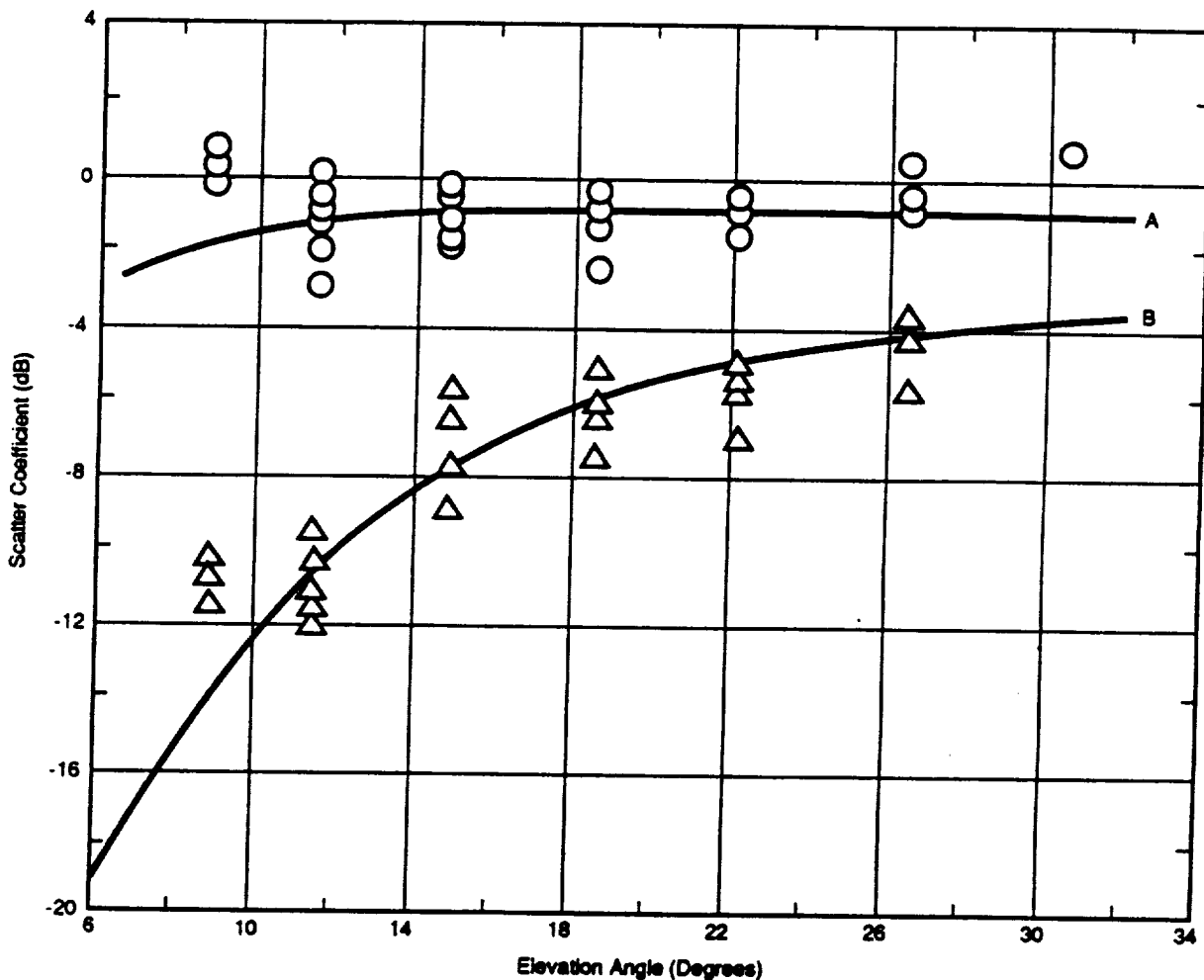


Figure 4 - Ocean mean scatter coefficient vs elevation angle for horizontal and vertical polarizations at 1.6 GHz; solid lines are product of plane-earth reflection coefficient and the divergence factor

- O - Horizontal polarization measurements
- Δ - Vertical polarization measurements
- A - Horizontal polarization predictions
- B - Vertical polarization predictions

Coefficients for horizontal and vertical antenna polarizations were measured in the ATS-6 experiments. Values for r.m.s. sea surface slopes of 3° and 12° are plotted versus elevation angle in Figure 6, along with predictions derived from a physical optics model [Staras, 1968]. Sea slope was found to have a minor effect for elevation angles above about 10°. The agreement between measured coefficients and those predicted for a smooth flat earth as modified by the spherical-earth divergence factor (Report 1008, eq. 12) increased as sea slope decreased. (The relation between r.m.s. sea surface slope and wave height is complex, but conversion can be performed [Karasawa and Shiokawa, 1984].)

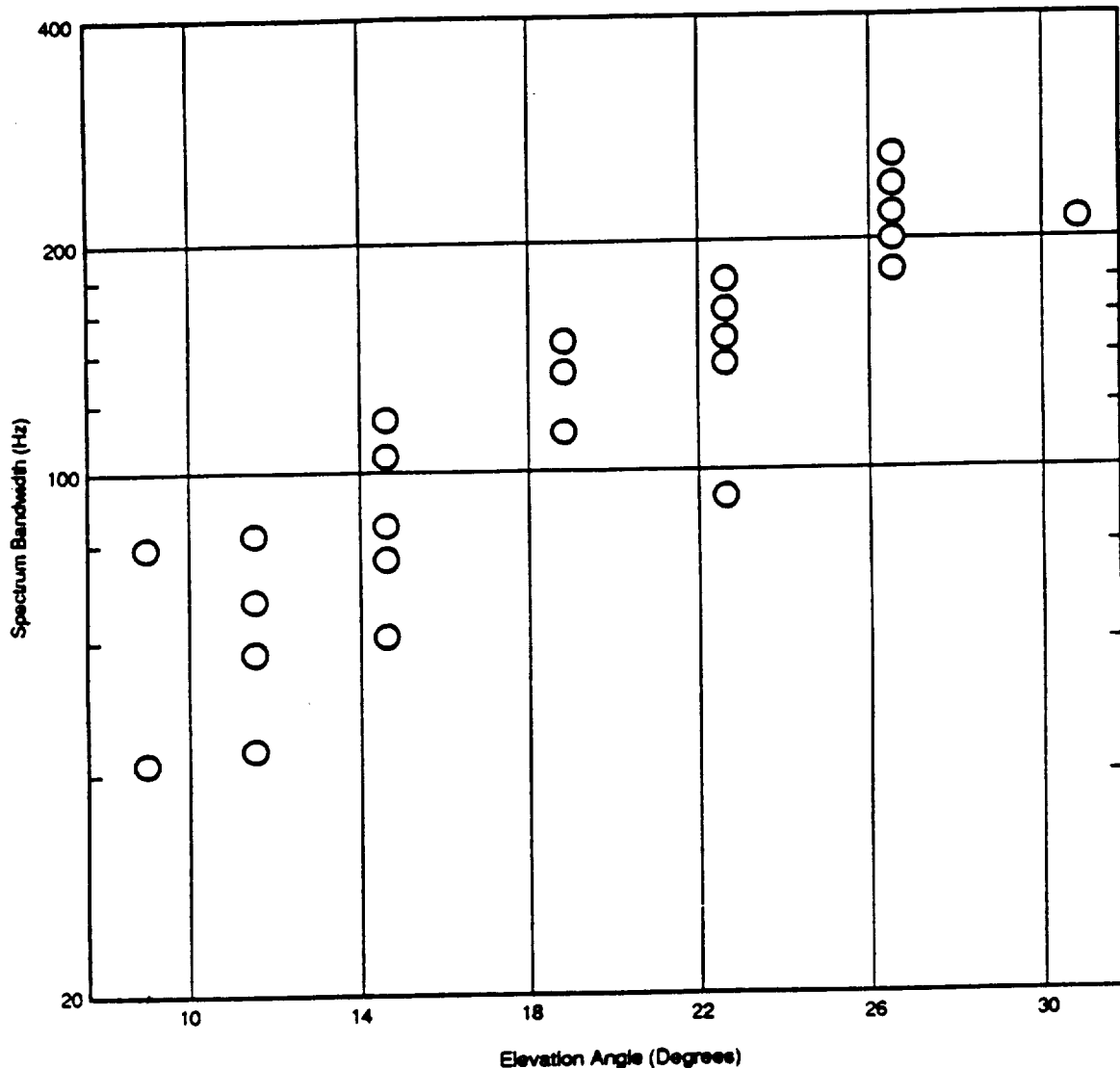


Figure 5 - Spectrum bandwidth (two-sided) of reflected waves vs elevation angle at 1.6 GHz

Table II - Multipath parameters from ocean measurements

Parameter	Measured Range	Typical value at specified elevation angle		
		8 deg	15 deg	30 deg
Mean square scatter coeff. (horizontal polarization)	-5.5 to -0.5 dB	-2.5 dB	-1 dB	-1 dB
Mean square scatter coeff. (vertical polarization)	-15 to -2.5 dB	-14 dB	-9 dB	-3.5 dB
Delay spread ² 3-dB value 10-dB value	.25 - 1.8 μs 2.2 - 5.6 μs	0.6 μs 2.8 μs	0.8 μs 3.2 μs	0.8 μs 3.2 μs
Coherence bandwidth ¹ (3-dB value)	70 to 380 kHz	160 kHz	200 kHz	200 kHz
Doppler spread ² : In-plane geometry 3-dB value 10-dB value	4 - 190 Hz 13 - 350 Hz	5 Hz 44 Hz 40 Hz*	70 Hz 180 Hz	140 Hz 350 Hz
Cross-plane geometry 3-dB value 10-dB value	79 - 240 Hz 180 - 560 Hz	63 Hz 144 Hz 88 Hz*	110 Hz 280 Hz	190 Hz 470 Hz
Decorrelation time ¹ (3-dB value)	1.3 - 10 msec	7.5 msec	3.2 msec	2.2 msec

*Data from multipath model (Report 884, § 4) for aircraft height of 10 km and aircraft speed of 1000 km/h.

¹One-sided.

²Two-Sided.

For most aeronautical systems, circular polarization will be of greater interest than linear. For the simplified case of reflection from a smooth earth (which should be a good assumption for elevation angles above 10°), circular copolar and cross-polar scatter coefficients (Γ_C and Γ_X , respectively) can be expressed in terms of the horizontal and vertical coefficients (Γ_h and Γ_v , respectively) by

$$\Gamma_C = (\Gamma_h + \Gamma_v)/2 \quad ; \quad \Gamma_X = (\Gamma_h - \Gamma_v)/2 \quad (3)$$

for either incident right-hand circular (RHC) or left-hand circular (LHC) polarization. The horizontal and vertical coefficients are complex-valued, in general. Therefore, phase information is required to apply eq. 3 to the curves in Figure 6.

Multipath data were collected in a series of aeronautical mobile-satellite measurements conducted over the Atlantic Ocean and parts of Europe [Hagenauer et al., 1987]. Figure 7 shows the measured mean and standard deviations of 1.6-GHz fade durations as a function of elevation angle for these flights. A crossed-dipole antenna with a gain of 3.5 dBi was used to collect these data. The aircraft flew at a nominal altitude of 10 km and with a nominal ground speed of 700 km/h.

4.4 Measurements of land-reflection multipath effects

Table III supplies multipath parameters measured during the ATS-6 flights over land [Schroeder et al., 1976]; parameter definitions are the same as for Table II. Land multipath signals were found to be highly nonstationary. No consistent dependence on elevation angle was established, perhaps because the ground terrain was highly variable (data were collected over wet and dry soil, marshes, dry and wet snow, ice, lakes, etc.). Figures 8a and 8b provide the mean-square scatter coefficients measured in the over-land tests, along with theoretical values (solid lines) from the physical optics model [Staras, 1968].

5. Irreducible error rate

Multipath fading in mobile channels gives rise to an irreducible error rate floor at which increases in the direct signal power do not reduce the corresponding error rate. Simulations of an aeronautical mobile-satellite link have been performed with a differentially-encoded minimum-shift-keyed signal [Davarian, 1988]. The composite (direct plus diffusely-reflected) signal was modeled with Rician statistics, and the reflected signal was suitably delayed with respect to the direct signal. The composite signal was differentially detected and a bit-error-rate test conducted.

The results indicated that the irreducible error rate is higher for an aeronautical mobile-satellite channel than for a land mobile-satellite channel. Increased delay of the multipath component caused the irreducible error rate to increase. Other studies [Hagenauer, 1987; Korn, 1989] support these results and show that an increase in multipath power or delay will increase the irreducible error rate.

Table III - Multipath parameters from land measurements

Parameter	Measured Range	Typical Value
Mean Square Scatter Coeff. (horizontal pol.)	-18 to 2 dB	-9 dB
Mean Square Scatter Coeff. (vertical pol.)	-21 to -3 dB	-13 dB
Delay spread ² (3-dB)	0.1 to 1.2 μ s	0.3 μ s
Delay spread ² (10-dB)	0.2 to 3 μ s	1.2 μ s
Coherence bandwidth ¹ (3-dB)	150 kHz to 3 MHz	600 kHz
Doppler spread ² (3-dB)	20 to 140 Hz	60 Hz
Doppler spread ² (10-dB)	40 to 500 Hz	200 Hz
Decorrelation time ¹ (3-dB)	1 to 10 msec	4 msec

¹One-sided.

²Two-sided.

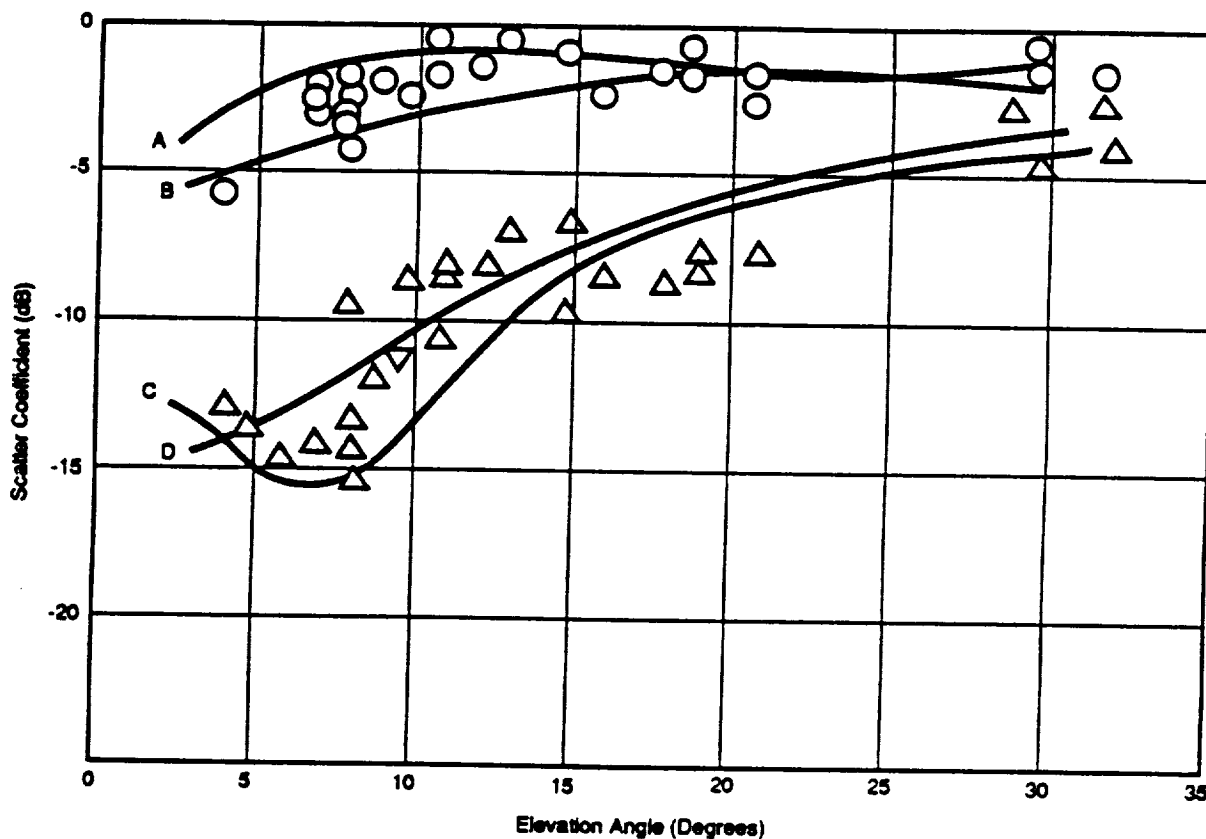


Figure 6 - Oceanic mean-square scatter coefficients vs elevation angle at 1.6 GHz

- O - Horizontal polarization measurements
- Δ - Vertical polarization measurements
- A - Horizontal polarization prediction, 3° slope
- B - Horizontal polarization prediction, 12° slope
- C - Vertical polarization prediction, 3° slope
- D - Vertical polarization prediction, 12° slope

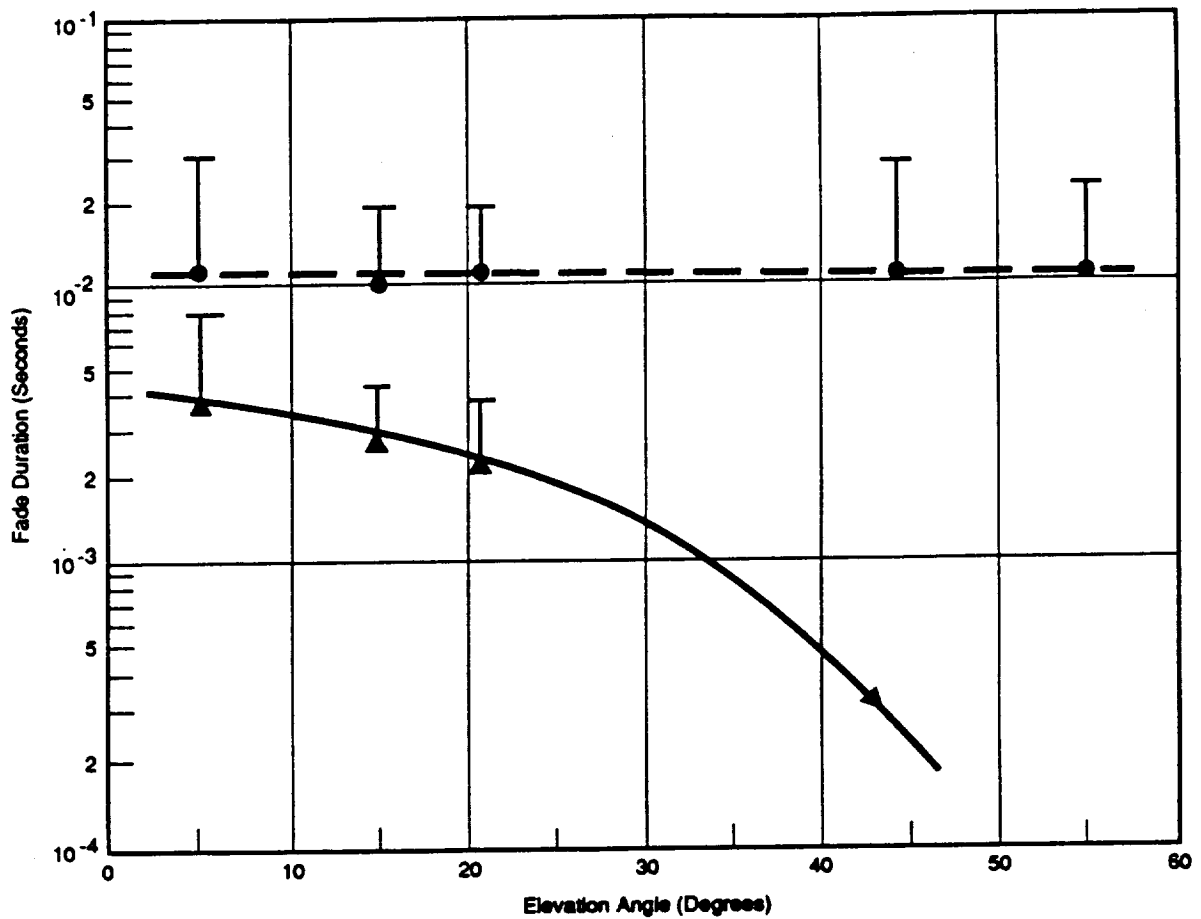


Figure 7 - Fade duration vs elevation angle for circular polarization at 1.6 GHz (antenna gain = 3.5 dBi); data collected over Atlantic Ocean and W. Europe

- Mean with 0 dB threshold
- ▲ Mean with -5 dB threshold
- T Standard deviation added

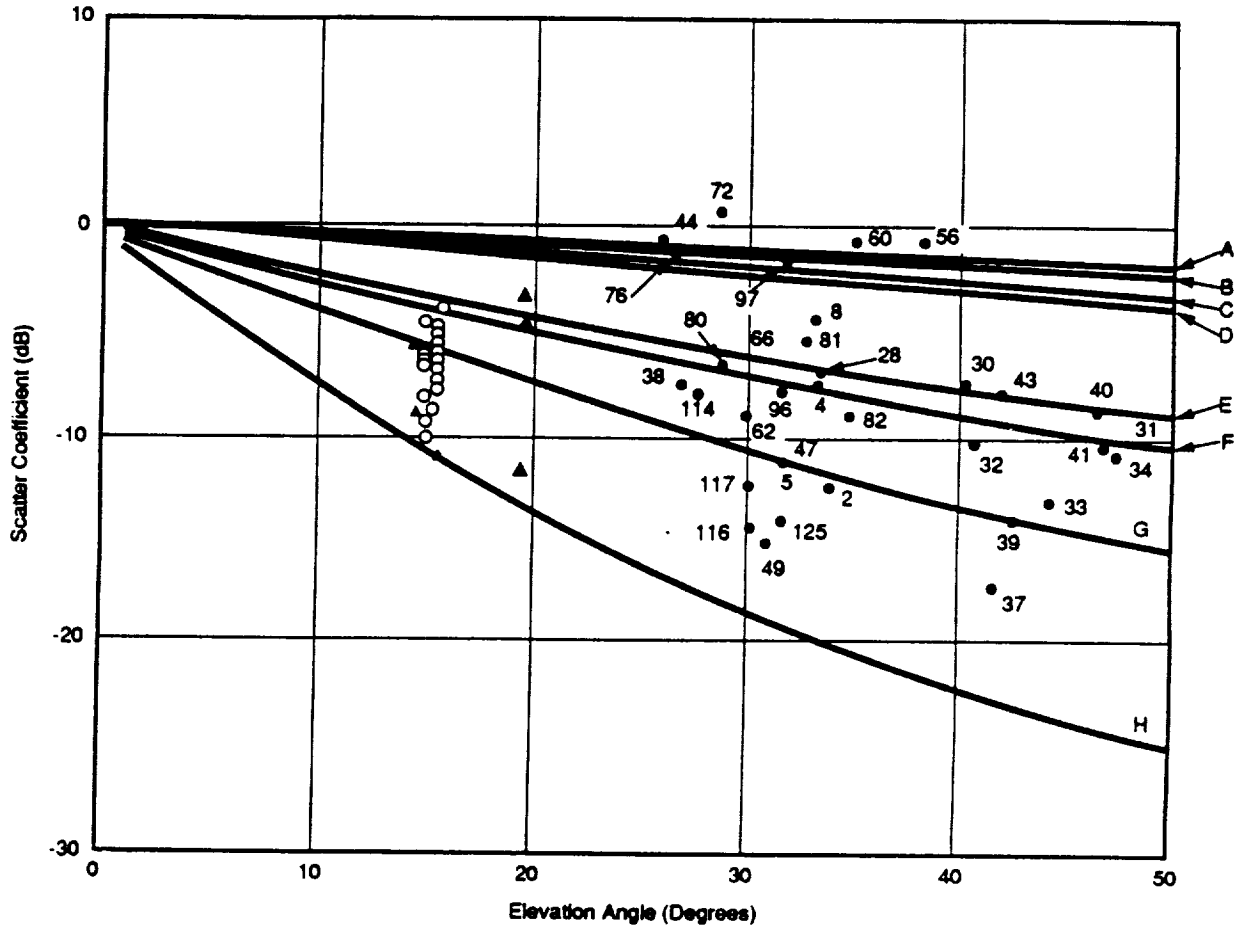


Figure 8a - Mean-square scatter coefficient for horizontal polarization vs elevation angle at 1.6-GHz; data collected over continental United States (numbers identify measurement runs)

- | | | | |
|----|-----------------------|----|---------------------|
| △ | ATS-5 summertime data | ○ | ATS-6 data |
| ○ | ATS-5 wintertime data | | |
| A: | Sea water | E: | Ice |
| B: | Fresh water | F: | Moderately dry soil |
| C: | Marsh | G: | Wet snow |
| D: | Slightly wet soil | H: | Dry snow |

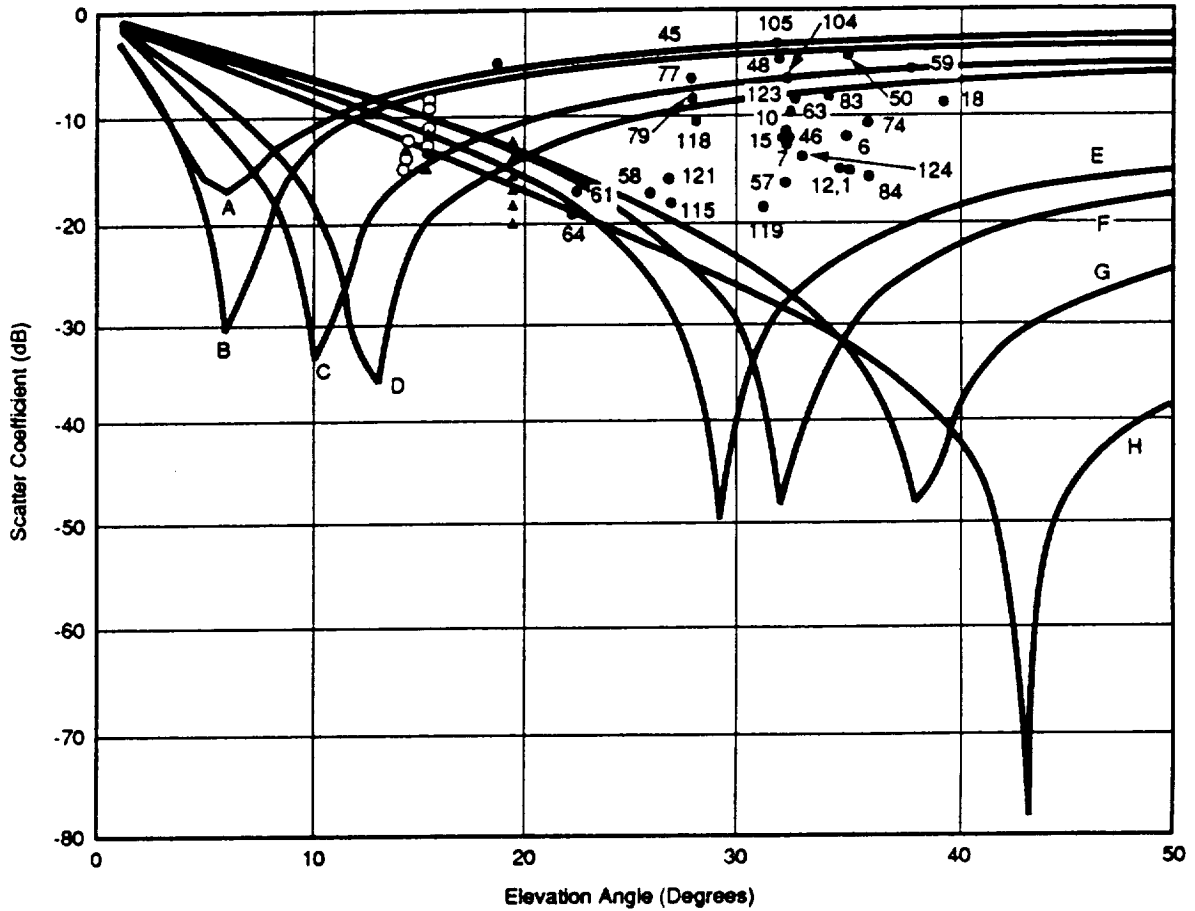


Figure 8b - Mean-square scatter coefficient for vertical polarization vs elevation angle at 1.6-GHz; data collected over continental United States (numbers identify measurement runs)

- | | | | |
|----|-----------------------|----|---------------------|
| Δ | ATS-5 summertime data | ○ | ATS-6 data |
| ○ | ATS-5 wintertime data | | |
| A: | Sea water | E: | Ice |
| B: | Fresh water | F: | Moderately dry soil |
| C: | Marsh | G: | Wet snow |
| D: | Slightly wet soil | H: | Dry snow |

REFERENCES

- DAVARIAN, F. [1988] Irreducible error rate in aeronautical satellite channels. *Electron.Lett.*, Vol. 24, 21, 1332-1333.
- HAGENAUER, J., NEUL, A., PAPKE, W., DOLAINSKY, F. and EDBAUER, F. [1987] The aeronautical satellite channel, DFVLR, May.
- KARASAWA, Y. and SHIOKAWA, T. [1984] Characteristics of L-band multipat fading due to sea surface reflection. *IEEE Trans.Ant.Prop.*, Vol. AP-32, 6, 618-623.
- KORN, I. [1989] Coherent detection of M-ary phase-shift keying in the satellite mobile channel. To be published in *IEEE Trans.Comm.*
- SCHROEDER, E.H., THOMPSON, A.D., SUTTON R.W., WILSON, S.G. and KUO, C.J [1976] Air traffic control experimentation and evaluation with the NASA ATS-6 satellite. The Boeing Company, Report No. FAA-RD-75-173, prepared for U.S. Dept. of Transportation. Vol. III, NTIS Accession No. D6-44048; Vol. V, NTIS Accession No. D6-44050, National Technical Information Service, Springfield, VA 22161, USA.
- SLOBIN, S.D. [1982] Microwave noise temperature and attenuation of clouds: Statistics of these effects at various sites in the United States, Alaska, and Hawaii. *Radio Sci.*, Vol. 17, 6, 1443-1454.
- STARAS, H. [1968] Rough surface scattering on a communication link. *Radio Sci.*, Vol. 3, 6, 623-631.
- SUTTON, R.W., SCHROEDER, E.H., THOMPSON, A.D., and WILSON, S.G. [1973a] ATS-5 multipath/ranging/digital data L-band experimental program: Program summary. The Boeing Company, Report No. FAA-RD-73-57, prepared for U.S. Dept. of Transportation. NTIS Accession No. D6-60176, National Technical Information Service, Springfield, VA 22161, USA.
- SUTTON, R.W., SCHROEDER, E.H., THOMPSON, A.D. and WILSON, S.G. [1973b] Satellite-aircraft multipath and ranging experiment results at L band. *IEEE Trans.Comm.*, Vol. COM-21, 5, 639-647.
- YASUNAGA, M., KARASAWA, Y., SHIOKAWA, T. and YAMADA, M. [1986] Characteristics of L-band multipath fading due to sea surface reflection in aeronautical satellite communications. *Trans.IECE* (Japan), Vol. E69, 10, 1060-1063.
- ZAKS, C. and ANDERSON, S. [1986] Aeronautical satellite data link measurement over the North Atlantic: Test results. *Proceedings*, Seventh Intl. Conf. on Digital Satellite Communications, Munich, FRG, May, 557-563.